Journal of Materials Chemistry B

Accepted Manuscript

ROYAL SOCIETY OF CHEMISTRY

www.rsc.org/materialsB

Journal Name Journal of Materials Chemistry B Dynamic Article Links ►

Cite this: DOI: 10.1039/c0xx00000x

www.rsc.org/xxxxxx

ARTICLE TYPE

Novel Biocompatible Double Network Hydrogels Consisting of Konjac Glucomannan with High Mechanical Strength and Free-shapeable Ability

Zhiyong Li, Yunlan Su*, Baoquan Xie, Xianggui Liu, Xia Gao and Dujin Wang*

Received (in XXX, XXX) Xth XXXXXXXXX 20XX, Accepted Xth XXXXXXXXX 20XX
DOI: 10.1039/b000000x

A novel physically linked double-network (DN) hydrogel based on natural polymer konjac glucomannan (KGM) and synthetic polymer polyacrylamide (PAAm) has been successfully developed. Polyvinyl alcohol (PVA) was used as macro-crosslinkers to prepare the PVA-KGM first network hydrogel with cycle freezing and thawing method for the first time. Subsequent introduction of a secondary PAAm network resulted in super-tough DN hydrogels. The resulting PVA-KGM/PAAm DN hydrogels exhibit a unique free-shapeable property, good cell adhesion property and excellent mechanical properties, which do not fracture upon loading up to 65 MPa and a strain above 0.98. The compressive strength and microstructure of the DN hydrogels were investigated as functions of acrylamide (AAm) content and freezing and thawing times. A unique embedded micro-network structure was observed in the PVA-KGM/PAAm DN gels and accounted for the significant improvement in compressive toughness. The fracture mechanism is discussed based on the yielding behaviour of these physically linked hydrogels.

1 Introduction

Tissue engineering, which is the use of a combination of material engineering and life science methods, seeks to create artificial constructs for regeneration of tissue.[1, 2] A common strategy adopted by tissue engineering is to isolate specific cells from a patient, and culture them on a three-dimensional (3D) scaffold. Subsequently, the scaffold is delivered to desired site of the patient's body to induce new tissue formation, which can be degraded over time.[2-4] Up to now, the synthesis of scaffold to satisfy all the requirements of tissue engineering is still a big challenge. Biocompatibility and biodegradability is essential for the scaffold materials, and the scaffold must also be strong enough so that it can resist the physical stress and support the patient's normal activities.[1]

Hydrogels, which are water-swollen polymer networks, are considered as innovative biomedical materials, due to their unique properties such as biocompatibility, responsiveness to various kinds of stimuli, ultralow surface friction and environment friendliness.[5-8] However, most of the natural and synthetic hydrogels exhibit a low mechanical strength, which severely restricts their biomedical applications.[9] Hence, many efforts have been focused on improving the mechanical strength of hydrogels to develop a tough hydrogel using for tissue engineering scaffold material. And several kinds of tough hydrogels have been prepared, such as double-network (DN) hydrogels,[10] slide-ring hydrogels,[11] nanocomposite hydrogels,[12] tetra-arm gels[13] as well as poly-functional initiating and cross-linking center (PFICC) hydrogels[14].

As a representative of tough hydrogel, DN hydrogel is characterized by a special network structure consisting of two types of polymer components with opposite physical natures: the minor component is a highly cross-linked rigid skeleton serving as a sacrificial bond, and the major component comprises a sparsely cross-linked ductile substance acting as a hidden length to sustain stress by large extension afterwards.[10, 15, 16] The conventional chemically linked DN hydrogels are generally synthesized via a two-step sequential free-radical polymerization process, in which a highly relative molecular mass neutral second polymer network is incorporated within a swollen heterogeneous first network.[10] According to the type of first network, the DN hydrogels are divided into polyelectrolyte-based DN hydrogel and neutral-based DN hydrogel. In contrast with the high strength and extensibility of polyelectrolyte-based DN hydrogels, most of neutral-polymer-based DN gels have modest strength and poor extensibility.[17] Until recently, Gong and co-workers developed a universal molecular stent method to prepare tough neutral-based DN hydrogels.[17, 18] However, this method increases the complexity of the hydrogel preparation process. In addition, it is required for an artificial scaffold material to form any specific complex shape depending on the desired site of patient. However, conventional DN hydrogels can be formed only in the limited shapes, such as a sheet or a disc, which could not meet the demands of different kinds of the patient's body. Till now, only three studies have shown to generate free-shaped DN gels.[19-21]

In this study, we present a simple method to synthesize tough neutral-polymer-based DN hydrogel without any complicated molecular stent, in which neutral polysaccharide konjac glucomannan (KGM) is introduced as the first network, and

neutral polyacrylamide (PAAm) is applied as the second network. The obtained hydrogel composites exhibit free-shapeable properties, good cell adhesion property and possess an extraordinarily high compressive strength of 65 MPa, which is much higher than that of any other neutral and natural polymer-based DN hydrogels early reported, such as the agar/PAAm DN gels (38 MPa)[21]. To the best of our knowledge, this is the first report for the synthesis of DN hydrogels with excellent mechanical based on the KGM. At the same time, the introduction of natural biopolymer, KGM, greatly improves the biocompatibility and biodegradability of the as-prepared tough PVA-KGM/PAAm hydrogel, which might open a new era of soft and wet materials as substitutes for articular cartilage and other tissues.

2. Materials and methods

2.1 Synthesis of single network hydrogels

1.0 g PVA (polymerization degree 1750, Sinopharm Chemical Reagent Co, Ltd., Shanghai, China) was added in 99.0 mL deionized water, the solution was heated to 96 ^{o}C and stirred for about 3 h to ensure the PVA was dissolved, to form a homogeneous transparent solution. 28.0 mL PVA solution and 2.0 mL $NH_3{\cdot}H_2O$ (25%, AR, Beijing Chemical Works) were added into a beaker with magnetic stirring. And then, 1.2 g KGM (98%, Hubei Tianyuan third Konjac Biotechnology Co., Ltd.) was added into the solution slowly with magnetic stirring. The mixture was heated at 50 ^{o}C for 3 hours. In the end, PVA-KGM hydrogels were fabricated with freezing-thawing (FT) by freezing the PVA-KGM solution in the mold in a refrigerator (-15 ^{o}C) for 6 h and thawing at ambient temperature. The ratio of PVA to KGM is 1 to 4.

2.2 Synthesis of double-network hydrogels

The PVA-KGM gel was immersed into a large amount of aqueous solution containing 0.01 mol% (respect to AAm) potassium persulfate, 0.01 mol% N,N'-Methylenebisacrylamide (MBAA, 99.0%, Aladdin Chemistry Co. Ltd) and different concentrations of Acrylamide (AAm, A.R., Aladdin Chemistry Co. Ltd) at 10 ^{o}C for 36 h (unless otherwise stated). The AAm monomer-swollen PVA-KGM gel was sandwiched by two glass plates and then heated at 50 ^{o}C for 24 h in a water bath to polymerize the AAm, leading to the formation of a PVA-KGM /PAAm DN hydrogel. The PVA-KGM/PAAm DN gel was immersed in water for one week with the water being changed once a day to remove the free substances.

2.3. Characterizations

2.3.1 Mechanical properties testing

The hydrogels were cut into cylindrical shaped specimens (15 mm in diameter) for compression testing and dumbbell shaped specimens standardized as DIN-53504 S3 for tensile testing. All tests were performed by using an Instron 3366 electronic universal testing machine (Instron Corporation, MA, USA). 10 kN load cells and cross head speeds of 4 mm min^{-1} were applied for compression tests. The compressive stress, σ_c, was calculated by σ_c=load/πr^2, where r is the original radius of the specimen. The strain (ε_c) under compression was defined as the change in the thickness (h) relative to the original thickness (h_0) of the free standing specimen, $\varepsilon_c = (h-h_0)/h_0$. Stress and strain between ε_c=0.1-0.2 were used to calculate the initial elastic modulus (Ec). At least three specimens per experimental point were tested in all mechanical measurements to obtain reliable values. The compressive strength for the DN hydrogels was defined as the compressive stress at ε_c = 98%. For tensile tests, 100 N load cells and the crosshead speeds of 80 mm min^{-1} was chose. The tensile stress σ_t was calculated using σ_t = load/tw (t and w are the initial thickness and width of the dumbbell shaped gel sample, respectively), and the fracture tensile stress (σ_b) is the tensile stress at which the sample breaks. The tensile strain (ε_t) is defined as the change in the length relative to the initial gauge length, and the fracture tensile strain (ε_b) is the tensile strain at which the sample breaks. Stress and strain between ε_t = 10 and 30 % were used to calculate the initial elastic modulus (E_t).

2.3.2 Rheological experiments

The gelation processes of KGM hydrogels are characterized by rheological experiments. The experiments were performed on a DHR-2 stress controlled rheometer (TA Instruments). Time sweep experiments were performed at 25^{o}C using a 25 mm parallel plate geometry. Samples were prepared by adding the KGM powders into the corresponding solutions (deionized water, PVA solution or PVA-$NH_3{\cdot}H_2O$ solution).

2.3.3 X-ray diffraction (XRD)

The PVA-KGM hydrogels obtained by the CFT method were dried at 40 ^{o}C, and then the dried films were characterized by a Rigaku D/max-2500 X'Pert instrument, operating with a monochromated Cu Kα radiation source at 40 kV/30 mA. Data were collected with a scanning speed of 4^{o} min^{-1} in the $10^{o}\leq 2\theta \leq 60^{o}$ range. Strong crystalline reflections in the 2θ range 18-21^{o} and two weak peaks centered at $2\theta \approx 28^{o}$ and 41^{o} correspond to the diffraction reflections of crystalline PVA.[22]

2.3.4 FT-IR characterizations

The samples used for FT-IR characterizations were dried at 50 ^{o}C until all water was removed. The FT-IR attenuated total refection (ATR) absorption spectra of the as-synthesized hydrogels were recorded using a Nicolet FT-IR 6700 spectrometer. A resolution of 4 cm^{-1} was chosen and 32 scans were accumulated.

2.3.5 Scanning Electron Microscopy (SEM)

The samples for SEM investigations were cut from the inner parts of hydrogel, and then they were plunged into liquid nitrogen for about 20 min. The frozen samples were subsequently freeze-dried in a FD-1B-50 vacuum freeze dryer (Beijing Boyikang Laboratory Apparatus Co., Ltd. Beijing, China) until all water was removed. The dried samples were cracked to exhibit their fresh surfaces. After being sputter-coated with Pt for 60 s, the morphologies of these fractured surfaces were observed with a JEOL JSM-6700 field emission scanning electron microscope with an accelerating voltage of 5 kV.

2.3.6 Swelling experiments

Swelling experiments were performed by immersing hydrogels in a large excess of water at room temperature to reach swelling equilibrium. The swelling ratio (SR) was calculated by the following equation, $SR = (W_s - W_d) / W_d \times 100\%$, where W_s and W_d are the weights of the swollen hydrogel and the corresponding dried hydrogel, respectively. The average of three measurements was taken for each sample.

2.3.7 Differential scanning calorimetry

The dry gel sample was placed in an aluminum pan. The differential scanning calorimetry measurements were performed under nitrogen atmosphere with a flow capacity of 50 ml/min by

a DSC Q2000 (TA, USA).

2.3.8 Cell cultivation

The gel specimens were die-cut into disks of radius 1.5 mm. Gel disks were sterilized in an autoclave (120 °C, 20 min) and then placed in a 24-well polystyrene (PS) tissue culture dish for cell culture. A mouse preosteoblast cells line (MC3T3-E1; Cell Resource Center, IBMS, CAMS/PUMC, China) suspension (2×10^4 cells/cm^2) was directly cultured on the gels without any modification. The cells were incubated at 37 °C in a humidified atmosphere of 5 % CO_2 for 3 days. Then the cytoskeleton of the cells was labeled with Alexa Fluor 488 fluorescein diacetate. Fluorescence images were taken with an Olympus FV1000 laser scanning confocal microscope (Olympus, Japan) with an excitation wavelength of 488 nm.

3. Results and discussion

3.1 First-network hydrogel

The natural biopolymer KGM is isolated from tubers of Amorphophallus konjac plants, which is water-soluble (at room temperature), easy gelation, and is biodegradable and biocompatible.[23, 24] The KGM hydrogels have been investigated widely because of their application in food and biomedical applications[25-28]. Unlike the existed normal methods to make KGM gelation, such as adding hydrogen bond cross-linking agent, adding synergistic complex agent, adding borax[29] and adding an alkaline substance (like calcium hydroxide and sodium carbonate),[30-32] in this work, a novel PVA-KGM hydrogel composite was firstly developed by cycle freezing and thawing (CFT) method in the presence of alkaline substance ($NH_3{\cdot}H_2O$). As shown in Scheme 1, $NH_3{\cdot}H_2O$ was first added into PVA solution to form an alkaline environment. Then KGM powder was slowly added into the PVA solution with magnetic stirring, and the PVA-KGM gel formed rapidly. The KGM would hydrolyze under alkaline condition and lose acetyl group, which is helpful for the formation of intermolecular hydrogen bond between the KGM and PVA chains. After heating 3 hours at 50 °C, the PVA-KGM gel was treated with CFT method at -15 °C and the PVA-KGM hydrogel was finally obtained.

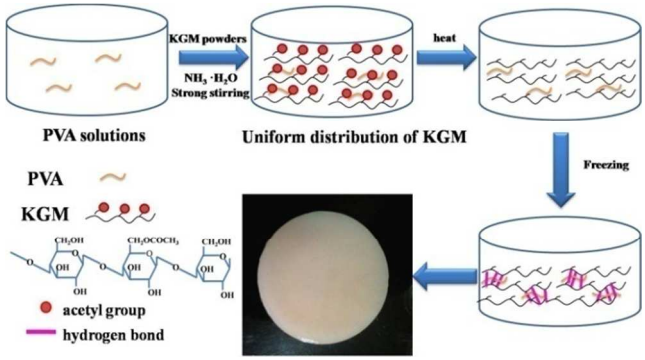

Scheme 1 Proposed mechanism for the formation of a PVA-KGM hydrogel.

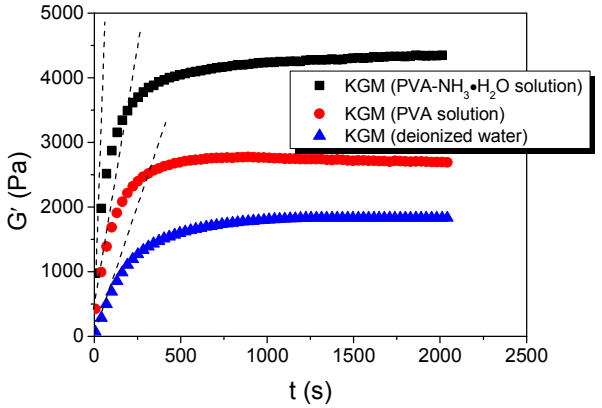

Fig. 1 Time dependence of G' for KGM solution at the frequency of 1 rad/s under 25 °C.

Rheological experiments are used to prove the formation of KGM hydrogel in this study. Figure 1 shows the time dependence of G' for KGM solution at the frequency of 1 rad/s under 25 °C. The G' increases sharply at the first stage, corresponding to the gelation process. After all the cross-links are formed and the gelation process is completed, one can see a plateau value of G' (G'p) independent of time. G'p has also been observed for other biopolymer gels which have obvious gelation processes. In addition, the effects of $NH_3{\cdot}H_2O$ and PVA on the formation of gels are investigated. As shown in Figure 1, the G' of the PVA-KGM hydrogel is higher than that of KGM hydrogel. However, the G' of the PVA-KGM hydrogel fabricated with $NH_3{\cdot}H_2O$ is the highest. Hence, both the PVA and $NH_3{\cdot}H_2O$ is in favour of increasing the degree of cross-linking of KGM hydrogel.

It is known that the first network is very important for the toughness of the DN gel. Hence, the structures and mechanical properties of the PVA-KGM hydrogels are investigated. As shown in Figure 2a, compared to pure KGM hydrogel, the PVA-KGM hydrogels have a higher compressive strength and initial elastic modulus, indicating that the existence of PVA is helpful to improve the mechanical properties of PVA-KGM hydrogel. And the improvement in mechanical properties of the PVA-KGM hydrogels suggests more intermolecular interaction formation with the addition of PVA. FT-IR characterizations were employed to understand these interactions, as shown in Figure 2b. There are two bands at 3262 cm^{-1} and 3290 cm^{-1}, which are corresponding to -OH stretching vibration of PVA and KGM, respectively. However, the PVA-KGM hydrogel has a band at 3279 cm^{-1}, which lies between 3262 cm^{-1} and 3290 cm^{-1}, suggesting the formation of hydrogen bond between the -OH (in PVA chains) and -NH_2 or -OH (in KGM chains).[31] The effect of CFT on the mechanical properties of PVA-KGM hydrogel has also been investigated (Figure 2c). The σ_c increases significantly with increasing the cycle number of freezing-thawing (FT), i.e. from 0.32 MPa at 1 FT cycle to 1.05 MPa at 4 cycles. The *Ec* of the PVA-KGM hydrogels also increases with increasing the number of FT cycles. In addition, CFT processing produces stable hydrogels that are physically cross-linked by the presence of crystalline regions.[33] In our system, XRD results (Figure 2d) show that the crystallinity of dried PVA-KGM hydrogel film increases from 33.3% (CFT-1) to 45.7% (CFT-4) with increasing the number of FT cycles. At the same time, the effect of FT cycle number on mechanical property of PVA-KGM hydrogel was also investigated by the rheological measurement (Supporting Figure S1). The increase of CFT number leads to a significant increase in G', indicating that CFT reinforces the network. In other words,

the density of physically cross-linked point increases with increasing the number of FT cycles, which resulting in the mechanical property enhancement with addition of PVA. Interestingly, the as-prepared PVA-KGM hydrogel contains 95% water, which is easily squeezed out, and there is no more recovery in the swelling property due to hydrogen-bond formation between KGM polymers (Supporting movie 1). At the same time, the hydrogel is easily broken into fragments under a modest compression of 1 MPa (at strain of ~ 70%).

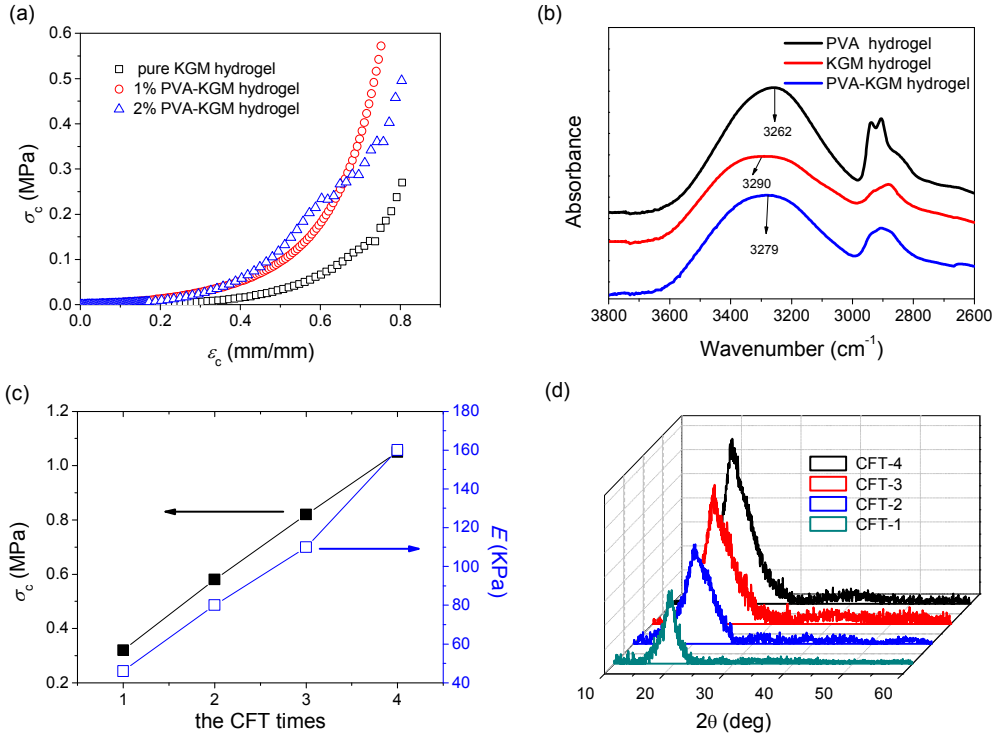

Fig. 2 Effects of PVA on the properties of KGM hydrogel: a) the compressive stress-strain curves of PVA-KGM hydrogel with different PVA content; b) FT-IR spectra of PVA, KGM and PVA-KGM hydrogel; c) the mechanical properties of PVA-KGM hydrogels prepared by different CFT times; d) the XRD of PVA-KGM hydrogels with different CFT times.

3.2 Double-network hydrogels

3.2.1 Morphology and structure

Based on the above physically cross-linked PVA-KGM hydrogel, the PVA-KGM/PAAm DN hydrogels were successfully obtained by polymerization. Fig. 3 compares the representative porous microstructures of first-network PVA-KGM hydrogels and PVA-KGM/PAAm DN hydrogels. As shown in the images, the PVA-KGM hydrogels have much bigger pore size than DN hydrogels. Specifically, the PVA-KGM hydrogel has an interconnected porous structure with pore sizes in the range of 40-50 μm. However, the DN hydrogels just have pores with sizes in the range of 0.3-5μm. Obviously, the PAAm chains lead to the formation of an embedded micro-network, which is believed to have significant influence on the mechanical properties of the DN hydrogels. Moreover, the microstructure of the DN hydrogels was also affected by CFT. The pore size of the hydrogel decreases from 5 to 0.3 μm with the increase of the CFT times (from 1 to 4).

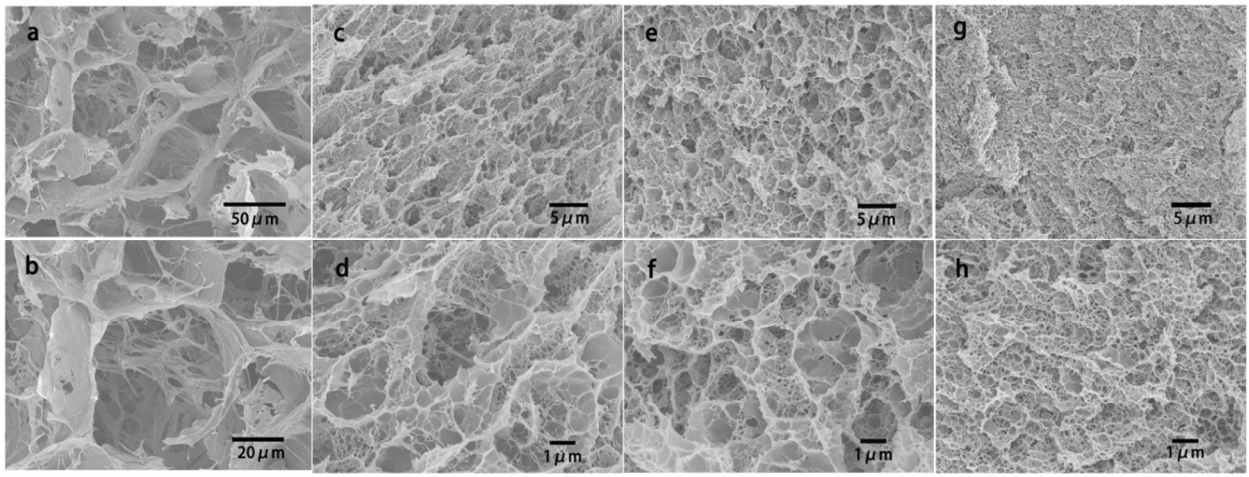

Fig. 3 SEM images of a PVA-KGM hydrogel (a and b) and the PVA-KGM/PAAm DN hydrogels (c–d: 1 CFT, e-f: 2 CFT, g-h: 4 CFT). The AAm concentration used for the preparation of DN hydrogel is 4 M.

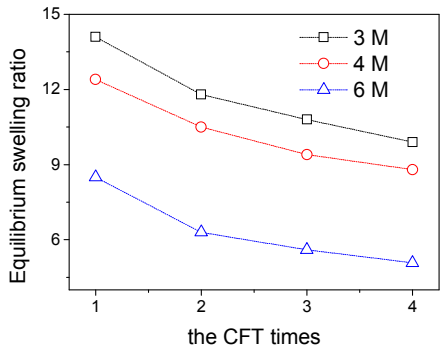

Fig.4 The equilibrium swelling ratios of DN hydrogels fabricated with different CFT times.

The equilibrium swelling ratios (ESR) of DN hydrogels are shown in Figure 4. It was found that the CFT times and AAm concentration could influence the ESR of the hydrogels. When the AAm concentration is constant, the ESR values of the DN hydrogel decrease with the increasing of CFT times, indicating a more rigid network formation or higher degree of cross-linking in the DN hydrogel fabricated with more CFT times. And this result could explain the SEM observations that the pore size of the hydrogel decreases with the increase of the CFT times. Moreover, the ESR values of the DN gels fabricated with high AAm content are lower than those of DN gels fabricated with low AAm content if the CFT times are the same.

3.2.2 Thermal properties

The thermal behaviour of PVA, PVA-KGM/PAAm DN hydrogels with different CFT times and KGM hydrogel were investigated by means of DSC analyses (Figure 5). PVA shows a relatively large melting peak at 227 °C, while a faintish melting peak of KGM occurred around 255 °C. Impressively, the DSC curves of DN hydrogels show only one endothermic peak between that of PVA and KGM hydrogel. The endothermic peak is attributed to the disintegration of the molecular chains. As shown in the Figure 5, the endothermic peak of DN hydrogels shifts to a higher temperature with the increase of CFT times. In addition, the peak shapes of PVA, KGM and DN hydrogel are different. In view of those changes of shape and location of the peaks in DSC curves, the different interactions established between the polymer chains are reasonable.

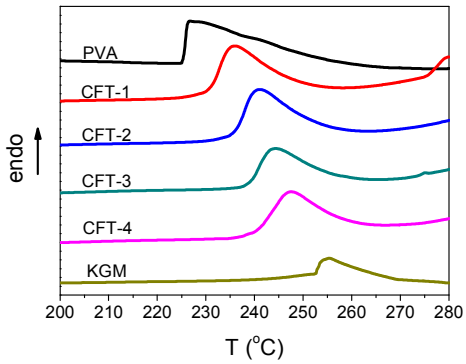

Fig. 5 The DSC curves of PVA hydrogel, PVA-KGM/PAAm DN hydrogel and KGM hydrogel.

3.2.3 Mechanical properties of the DN hydrogel

As shown in Figure 6, PVA-KGM/PAAm DN hydrogels exhibit free-shapeable properties and extraordinary mechanical property. Because of the good water-soluble property (at room temperature) and easy gelation, PVA-KGM/PAAm DN gels can be readily adapted to different complex shapes, such as fishes (Figure 6a) and column (Figure 6b). And the hydrogels are very tough, withstanding high-level deformations of bending (Figure 6c), warping (Figure 6d) and compression (Figure 6e) without any observable damage. Particularly, the hydrogels quickly recover to their initial shapes after the release of load, indicating that the gels exhibit excellent shape-recovery property. In contrast with PVA-KGM hydrogel, impressively, the PVA-KGM/PAAm DN hydrogel can hold water strongly even under the pressure as high as 65 MPa, and completely recover its original shape after the compression at a strain of 98% (Supporting movie 2).

The compressive properties of the DN hydrogels have also been investigated quantitatively. Figure 7a shows the typical compressive stress-strain curves of PVA-KGM gel, PAAm gel and their composite PVA-KGM/PAAm DN hydrogel. It is obvious that the PVA-KGM/PAAm DN hydrogel shows a different stress-strain profile compared with individual PVA-KGM and PAAm hydrogel. The DN hydrogel shows an extraordinarily high compressive strength of 30 MPa, which is more than 93 times higher than that of PVA-KGM hydrogel (0.32 MPa), and almost 38 times than that of the PAAm hydrogel (0.79 MPa). Similarly, the effect of CFT times on the mechanical properties of PVA-KGM/PAAm DN hydrogels was also investigated. As shown in Figure 7b, the σ_c increases significantly with increasing the number of FT cycles, i.e. from 30 MPa at 1 FT cycle to 65 MPa at 4 FT cycles. This extraordinarily high compressive strength (65 MPa) is about 2 times larger than that of the poly(2-acrylamido-2-methyl-1-propanesulfonic acid) (PAMPS)/PAAm DN hydrogel (21.0 MPa) as reported in the literature[10], and also significantly higher than most of the natural polymer-based DN hydrogels[15, 34]. Hence, this tough hydrogel has potential capability to be used as cartilage (exhibiting a compressive fracture stress of 36 MPa) and bone tissue engineering scaffold. Figures 7c and d also illustrate very large increase in toughness and strength with increasing the AAm monomer concentration used to prepare the second network, indicating that the toughness and strength increase at any CFT time. For example, when the FT time is one, ε_c increases from 10 MPa at 3 M to 30 MPa at 6 M AAm, and E_c increases from 50 kPa at 3 M to 200 kPa at 6 M AAm.

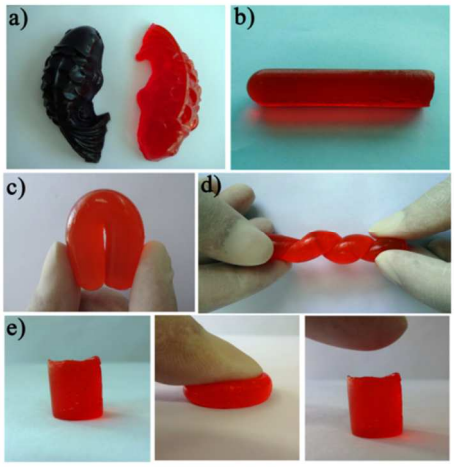

Fig. 6 PVA-KGM/PAAm DN hydrogels show free-shapeable properties and extraordinary mechanical toughness: a) two fishes with different colors (black and red ink was used respectively); b) a columnar hydrogel; c) bending; d) warping; e) compression. The AAm concentration used for the preparation of DN hydrogel is 3 M and the CFT is one time.

Extensive studies have shown that the toughness of DN hydrogel is thought to be derived mostly from the scission and unloading of first network strands. The high toughness occurs when the first network is more tightly cross-linked than the second network. The greater the toughness of the first network is, the more energy can be dissipated during the fracture of the DN gel.[35] In this study, CFT can improve the degree of cross-linkage, which contributes to the toughness of the first network, and results that the DN hydrogels have a much higher compressive strength. As mentioned above, both the σ_c and Ec increase with the increasing of CFT times. Moreover, the rheological properties of the PVA-KGM/PAAm DN hydrogels were also measured to prove it (Supporting Figure S2). And it is indicated that the increase of CFT leads to a significant increase in G'. Both the G' and the linear viscoelastic region of the DN hydrogel are much bigger than those of the PVA-KGM hydrogel (Supporting Figures S1 and S2), indicating that the DN hydrogel has a more perfect network. In addition, the degree of cross-linking of the second network is also important for the strength of DN hydrogel. The lower the cross-linking density of the second network is, the stronger the DN hydrogels are (Supporting Figure S3).

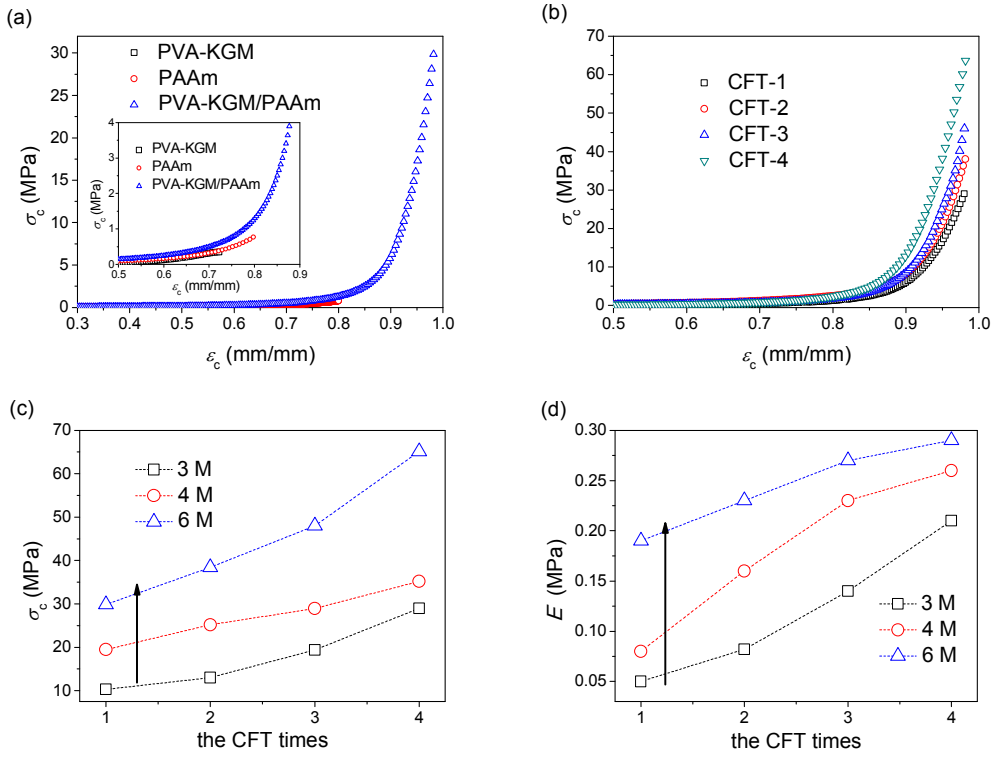

Fig. 7 a) The compressive stress-strain cures of PVA-KGM, PAAm and PVA-KGM/PAAm hydrogels (the PVA-KGM and PVA-KGM/PAAm DN hydrogels were fabricated by 1 FT); b) the compressive stress–strain curves of PVA-KGM/PAAm DN hydrogels prepared by different CFT times; c-d) the effect of AAm concentration in the feed on the fracture stress (c) and the elastic modulus (d) of PVA-KGM/PAAm DN hydrogels.

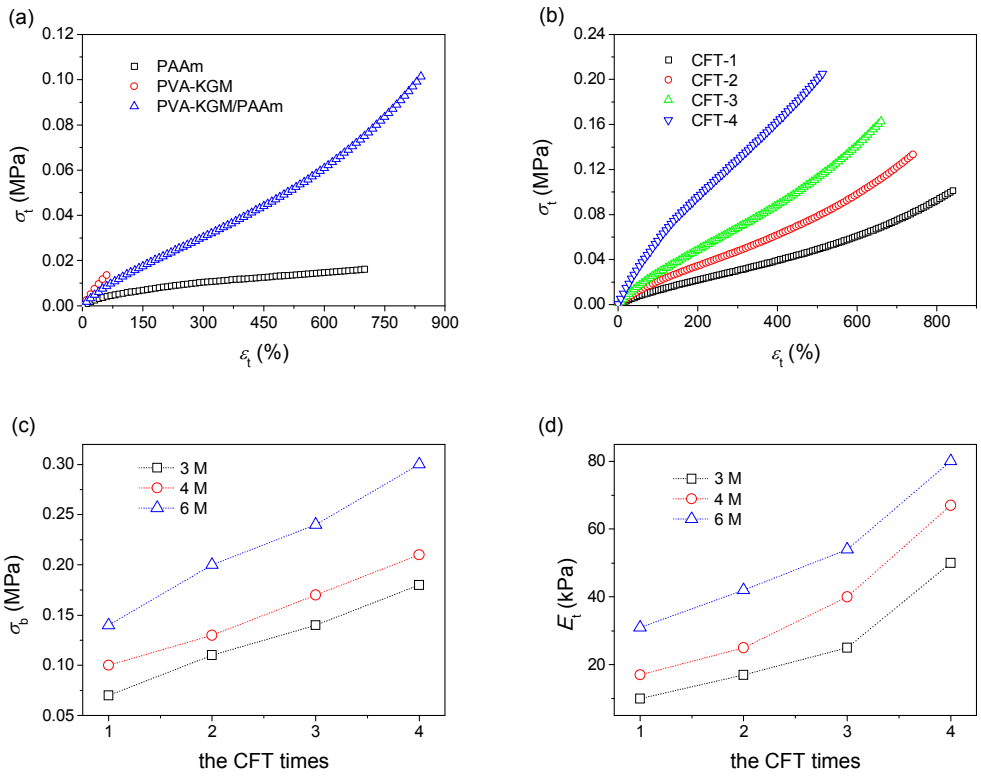

Fig. 8 a) The tensile stress-strain cures of PAAm, PVA-KGM, and PVA-KGM/PAAm hydrogels (the PVA-KGM and PVA-KGM/PAAm DN hydrogels were fabricated by 1 FT); b) the tensile stress–strain curves of PVA-KGM/PAAm DN hydrogels prepared by different CFT times; c-d) the effect of AAm concentration in the feed on the tensile fracture stress (c) and the elastic modulus (d) of PVA-KGM/PAAm DN hydrogels.

The tensile properties of the DN hydrogels have also been investigated (Figure 8). Figure 8a shows the tensile stress-strain curves of PAAm hydrogel, PVA-KGM hydrogel and PVA-KGM/PAAm DN hydrogel. As shown in the figure, the PVA-KGM/PAAm DN hydrogel exhibits a high tensile strength of 0.10 MPa, which is more than 7 times higher than that of PVA-KGM hydrogel (0.013 MPa), and almost 6 times higher than that of the PAAm hydrogel (0.016 MPa). Figure 8b shows the tensile stress-strain curves of PVA-KGM/PAAm DN hydrogels at the AAm concentration of 4 M. The σ_b increases with increasing the number of FT cycles, however, the ε_t decreases. Figures 8c and 8d show the σ_b and E_t of the DN hydrogels fabricated with different CFT times and different AAm concentration. With the increase of CFT times, σ_b (Fig. 8c) and E_t (Fig. 8d) of the DN hydrogels increase. At the same time, σ_b (Fig. 8c) and E_t (Fig. 8d) of the DN hydrogels also increase with the increase of C_M. For example, σ_b increases from 0.07 MPa at 3 M (1 FT) to 0.30 MPa at 6 M AAm (4 FT), and E_t increases from 10 kPa at 3 M (1 FT) to 80 kPa at 6 M AAm (4 FT).

3.3 Possible fracture mechanism of the PVA-KGM/PAAm double-network hydrogels

Meanwhile, some other compressive experiments were conducted to investigate the effect of the PVA, KGM and PAAm on compressive fracture of the DN hydrogels. First of all, the PVA-KGM/PAAm DN hydrogels show much higher compressive strength (about 3 times) and initial elastic modulus than those of the KGM/PAAm DN hydrogel (Figure 9a and 9b). In addition, the compression mechanical properties of PVA/PAAm hydrogel are given (Figure 9c). And the σ_c of PVA/PAAm hydrogel is much lower than that of KGM/PAAm and PVA-KGM/PAAm DN hydrogel. In a word, the combinations of PVA and KGM in the first network hydrogel play a key role for the extraordinary high mechanical properties of DN hydrogel. And the PVA chains may act as a cross-linking agent in the first network hydrogel system and play a reinforcement role through physical entanglements and hydrogen bonding among the PVA chains, KGM chains and the PAAm network in the DN network. These physical crosslinks are similar with host-guest interactions, which have also been used to prepare hydrogel.[36]

The cyclic compression experiments were also used to further investigate the possible fracture mechanism. Seen in Figure 10a, the compressive strength of the second upon loading is lower than that of the first upon loading at the same strain, indicating that there are some structural damages during the first upon loading. And a cyclic compressive test shows that the PVA-KGM/PAAm DN hydrogel nearly recovers its original shape after a tenth compressive deformation up to 90% strain. Moreover, the loading/unloading curves of PVA-KGM/PAAm DN gels show typical hysteresis. As shown in Figure 10b, the stress-strain curves almost overlap except for the first run, suggesting that no significant irrecoverable damage has been done to the hydrogel network except the first loading upon. And the hysteresis is similar with the PAMPS/PAAm DN hydrogels, where the hysteresis corresponds to the break of the PAMPS network upon loading.[37-39] In this work, it is reasonable to hypothesize that the hysteresis behaviour of the PVA-KGM/PAAm DN hydrogel upon loading/unloading implies the fracture of the PVA-KGM network. Furthermore, the large hysteresis also indicates that the DN gels could accumulate the internal damage before their macroscopic fracture through the connection of the soft second network to the fragments of the brittle first network.[5, 38]

Based on the above analysis, we presume a possible fracture mechanism for the PVA-KGM/PAAm DN hydrogels (Figure

10c). As shown in Fig. 10c (1), the PVA-KGM first network is physically cross-linked by physical entanglement and noncovalent bonds, which includes intramolecular and intermolecular hydrogen bond. Specifically, the intramolecular hydrogen bonds form in KGM chain or PVA chain, and the intermolecular hydrogen bonds form between KGM and KGM chains, PVA and PVA chains or KGM and PVA chains. Upon applying strains on the gels, the PVA-KGM first-network starts to be damaged. The KGM chains and the hydrogen bonds will be damaged, while the KGM chains start to unzip (indicating by the blue frame) as well (Figure 10c (2)).[40] As the strain increases, the PVA-KGM network gradually becomes homogeneous. In the end, the PVA-KGM first-network ruptures into small clusters and dissipates energy, leading to the robust compressive toughness (65 MPa) and extraordinary extensibility.[5, 21]

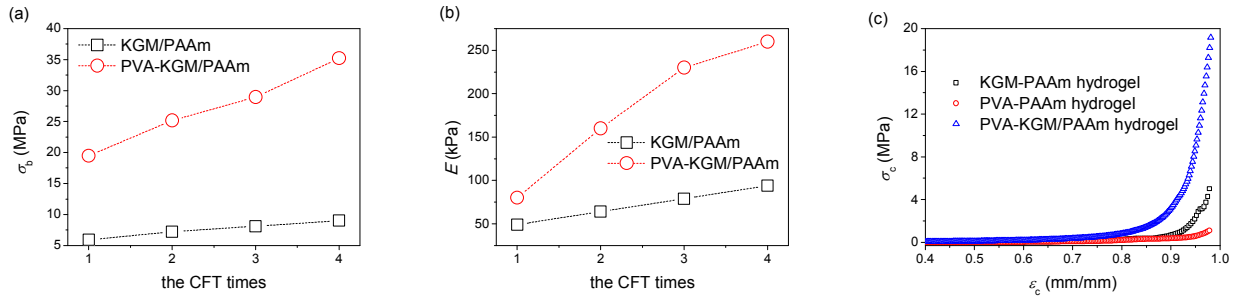

Fig. 9 (a-b) The effect of PVA on the compressive strengths (a) and elasticity modulus (b) of the PVA-KGM/PAAm DN hydrogel. (c) The compressive stress-strain curves of KGM/PAAm hydrogel, PVA/PAAm hydrogel and PVA-KGM/PAAm DN hydrogel. The AAm concentration used for the preparation of DN hydrogel is 4 M.

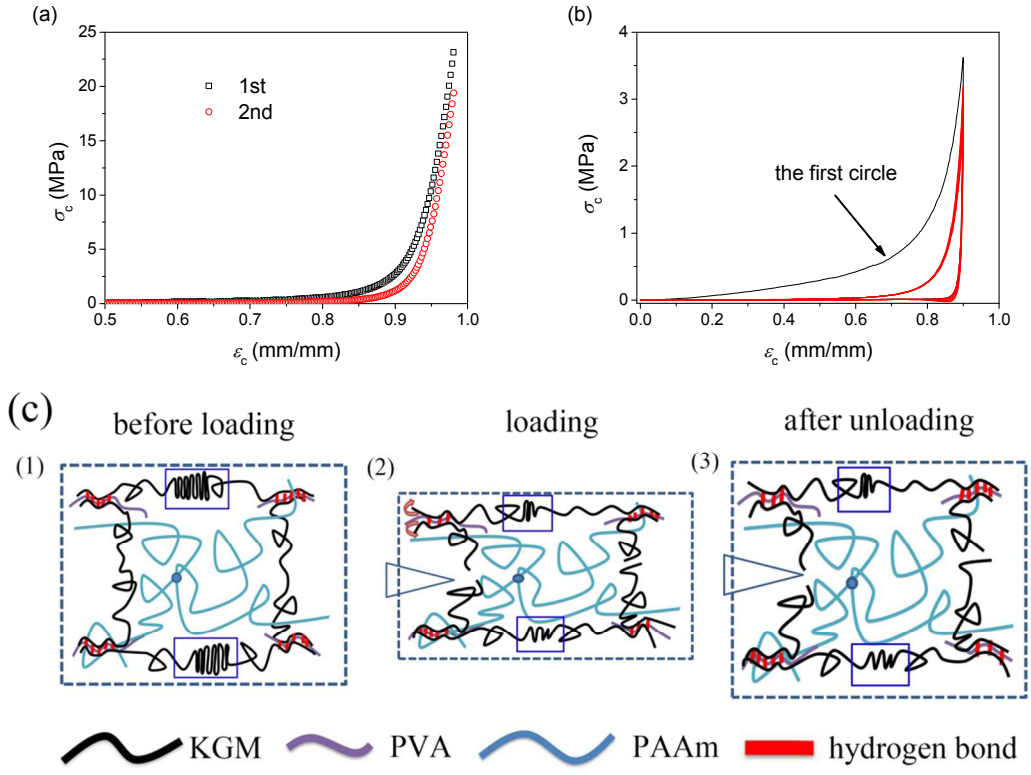

Fig. 10 a) The first and second compression stress–strain curves of a PVA-KGM/PAAm DN hydrogel under a continuous compression tests. b) Stress–strain curves of a PVA-KGM/PAAm DN hydrogel under repeated compression (ten times) tests. c) Schematic illustrations of the fracturing mechanisms of the PVA-KGM/PAAm DN hydrogels. The AAm concentration used for the preparation of DN hydrogel is 4 M and the CFT is 2 times.

3.4 Cell adhesion of the double-network hydrogel

Both PVA hydrogel and PAAm hydrogel have not been considered to be strong cell adhesion materials. And many actions have been taken to improve their cell adhesion properties, for example, modifying the hydrogels by incorporation of bio-active molecules[41] or bio-active inorganic particles[42]. West and co-workers modified the PVA hydrogel with the cell-adhesive peptide RGDS, and the obtained PVA hydrogel was found to support the attachment and spreading of fibroblasts in a dose-dependent manner.[41] Fu et al. have reported a novel magnetic nano-hydroxyapatite/PVA composite hydrogels with controllable cell adhesion and proliferation properties.[43] And in our previous work, PAAm/HAp composite hydrogel with good cell adhesion properties have also been obtained successfully.[8]

Moreover, DN approaches to modify hydrogel characteristics, which are helpful for improving cell adhesion properties, could also be important because supplemental changes compared to the single network hydrogels depend on the other component and DN structures. Recently, Gong and co-workers have introduced biopolymer (such as sodium hyaluronate and chondroitin sulphate) into the DN hydrogel, which enhanced the cell adhesion property of the DN hydrogel.[18] To further investigate the potential of the PVA-KGM/PAAm DN hydrogels as scafford for tissue engineering, we cultured mouse preosteoblast cells on the hydrogels. Typical confocal fluorescent microscopy images of mouse preosteoblast cells cultured for 3 days are shown in Figure 11. No cell is observed on the surface of PAAm hydrogel and PVA hydrogel. In contrast, on the KGM hydrogel, PVA-KGM hydrogel and PVA-KGM/PAAm DN hydrogel surfaces, a great number of cells can be observed. What's more, on the PVA-KGM hydrogel and PVA-KGM/PAAm DN hydrogel surfaces, osteoblasts spread and appeared in fusiform. These results indicate that the presence of KGM in the DN hydrogel enhances the cell adhesion on the composite hydrogel surface.

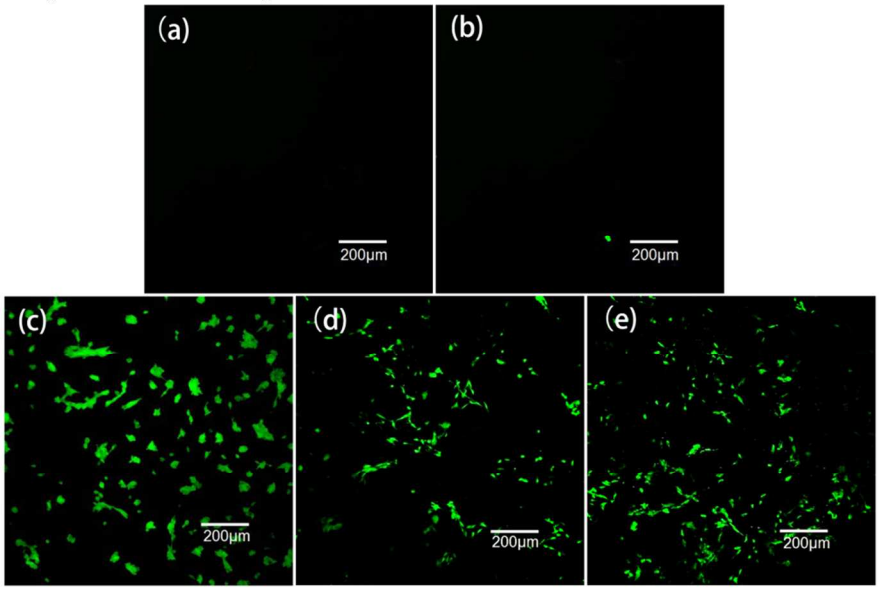

Fig.11 Confocal fluorescent microscopic images of mouse preosteoblast cells cultured for 3 days on the hydrogels. (a) PAAm hydrogel, (b) PVA hydrogel, (c) KGM hydrogel, (d) PVA-KGM hydrogel and (e) PVA-KGM/PAAm DN hydrogel. The AAm concentration used for the preparation of DN hydrogel is 4 M and the CFT is 1 time.

Conclusions

In conclusion, novel biocompatible and mechanically strong DN hydrogels were synthesized by exquisite combinations of natural polymers (KGM) and synthetic polymers (PAAm). The resulting PVA-KGM/PAAm DN hydrogels exhibit high mechanical strength (compressive toughness 65 MPa) and excellent shape recoverability. The hydrogels can also be easily adapted to different complex shapes and show good cell adhesion property. Moreover, the microstructures and the compressive toughness of the DN hydrogels are easily tunable based on the CFT times, the AAm concentration and cross-linker content. The synergistic effect between the physical entanglements and hydrogen bond provides excellent connections of the PVA polymers and the PAAm network, which result in the extraordinarily compressive toughness and extensibility of the PVA-KGM/PAAm DN hydrogels. In addition, the biodegradability and biocompatibility of the DN hydrogel can be further improved by optimizing the chemical compositions of the second network and the cross-linking component. In a word, the combination of excellent mechanical properties and free-shapeable ability, along with good cell adhesion property, makes the PVA-KGM/PAAm DN hydrogel materials have potential applications for load-bearing artificial soft tissues.

Acknowledgements

This work is financially supported by International S&T Cooperation Program of China (Grant No. S2013DFG52300). The authors thank Professor Changcheng He at Beijing Normal University for helpful discussions and suggestions.

Notes and references

Beijing National Laboratory for Molecular Sciences, Key Laboratory of Engineering Plastics, Institute of Chemistry, Chinese Academy of Sciences, Beijing 100190, P. R. China. Fax: +86-10-82612857; Tel: +86-10-82618533; E-mail: ylsu@iccas.ac.cn, djwang@iccas.ac.cn

† Electronic Supplementary Information (ESI) available: [The frequency (a) and amplitude (b) dependence of storage modulus G′ of the PVA-KGM hydrogels; The frequency (a) and amplitude (b) dependence of storage modulus G′ of the PVA-KGM/PAAm DN hydrogels; The effect

of MBAA concentration on the compressive strength of the PVA-KGM/PAAm DN hydrogel]. See DOI: 10.1039/b000000x/

‡ Footnotes should appear here. These might include comments relevant to but not central to the matter under discussion, limited experimental and spectral data, and crystallographic data.

1 K. Rezwan, Q. Chen, J. Blaker and A. R. Boccaccini, *Biomaterials*, 2006, **27**, 3413-3431.

2 J. F. Mano, R. A. Sousa, L. F. Boesel, N. M. Neves and R. L. Reis, *Compos. Sci. Technol.*, 2004, **64**, 789-817.

3 D. Williams, *Mater. Today*, 2004, **7**, 24-29.

4 H. Shin, S. Jo and A. G. Mikos, *Biomaterials*, 2003, **24**, 4353-4364.

5 Q. Wang, R. Hou, Y. Cheng and J. Fu, *Soft Matter*, 2012, **8**, 6048.

6 K. L. Spiller, Y. Liu, J. L. Holloway, S. A. Maher, Y. Cao, W. Liu, G. Zhou and A. M. Lowman, *J. Control. Release*, 2012, **157**, 39-45.

7 A. Vashist, S. Shahabuddin, Y. K. Gupta and S. Ahmad, *J. Mater. Chem. B*, 2013, **1**, 168.

8 Z. Li, Y. Su, B. Xie, H. Wang, T. Wen, C. He, H. Shen, D. Wu and D. Wang, *J. Mater. Chem. B*, 2013, **1**, 1755.

9 T. Huang, H. G. Xu, K. X. Jiao, L. P. Zhu, H. R. Brown and H. L. Wang, *Adv. Mater.*, 2007, **19**, 1622-1626.

10 J. P. Gong, Y. Katsuyama, T. Kurokawa and Y. Osada, *Adv. Mater.*, 2003, **15**, 1155-1158.

11 Y. Okumura and K. Ito, *Adv. Mater.*, 2001, **13**, 485-487.

12 K. Haraguchi and T. Takehisa, *Adv. Mater.*, 2002, **14**, 1120.

13 T. Sakai, T. Matsunaga, Y. Yamamoto, C. Ito, R. Yoshida, S. Suzuki, N. Sasaki, M. Shibayama and U.-i. Chung, *Macromolecules*, 2008, **41**, 5379-5384.

14 J. Liu, C. Chen, C. He, J. Zhao, X. Yang and H. Wang, *ACS Nano*, 2012, **6**, 8194-8202.

15 C. Fan, L. Liao, C. Zhang and L. Liu, *J. Mater. Chem. B*, 2013, **1**, 4251.

16 H. Yin, T. Akasaki, T. Lin Sun, T. Nakajima, T. Kurokawa, T. Nonoyama, T. Taira, Y. Saruwatari and J. Ping Gong, *J. Mater. Chem. B*, 2013, **1**, 3685.

17 T. Nakajima, H. Sato, Y. Zhao, S. Kawahara, T. Kurokawa, K. Sugahara and J. P. Gong, *Adv. Funct. Mater.*, 2012, **22**, 4426-4432.

18 Y. Zhao, T. Nakajima, J. J. Yang, T. Kurokawa, J. Liu, J. Lu, S. Mizumoto, K. Sugahara, N. Kitamura, K. Yasuda, A. U. Daniels and J. P. Gong, *Adv. Mater.*, 2014, **26**, 436-442.

19 T. Nakajima, N. Takedomi, T. Kurokawa, H. Furukawa and J. P. Gong, *Polym. Chem.*, 2010, **1**, 693.

20 J. Saito, H. Furukawa, T. Kurokawa, R. Kuwabara, S. Kuroda, J. Hu, Y. Tanaka, J. P. Gong, N. Kitamura and K. Yasuda, *Polym. Chem.*, 2011, **2**, 575.

21 Q. Chen, L. Zhu, C. Zhao, Q. Wang and J. Zheng, *Adv. Mater.*, 2013, **25**, 4171-4176.

22 R. Ricciardi, F. Auriemma, C. Gaillet, C. De Rosa and F. Lauprêtre, *Macromolecules*, 2004, **37**, 9510-9516.

23 X. Ye, J. F. Kennedy, B. Li and B. J. Xie, *Carbohydr. Polym.*, 2006, **64**, 532-538.

24 Y. Enomoto-Rogers, Y. Ohmomo and T. Iwata, *Carbohydr. Polym.*, 2013, **92**, 1827-1834.

25 L.-G. Chen, Z.-L. Liu and R.-X. Zhuo, *Polymer*, 2005, **46**, 6274-6281.

26 H. Yu and C. Xiao, *Carbohydr. Polym.*, 2008, **72**, 479-489.

27 C. Liu, Y. Chen and J. Chen, *Carbohydr. Polym.*, 2010, **79**, 500-506.

28 Z. L. Liu, H. Hu and R. X. Zhuo, *J. Polym. Sci. A: Polym. Chem.*, 2004, **42**, 4370-4378.

29 S. Gao, J. Guo and K. Nishinari, *Carbohydr. Polym.*, 2008, **72**, 315-325.

30 P. Fitzpatrick, J. Meadows, I. Ratcliffe and P. A. Williams, *Carbohydr. Polym.*, 2013, **92**, 1018-1025.

31 X. Xu, B. Li, J. F. Kennedy, B. J. Xie and M. Huang, *Carbohydr. Polym.*, 2007, **70**, 192-197.

32 L. Huang, R. Takahashi, S. Kobayashi, T. Kawase and K. Nishinari, *Biomacromolecules*, 2002, **3**, 1296-1303.

33 L. Zhang, J. Zhao, J. Zhu, C. He and H. Wang, *Soft Matter*, 2012, **8**, 10439-10447.

34 A. Nakayama, A. Kakugo, J. P. Gong, Y. Osada, M. Takai, T. Erata and S. Kawano, *Adv. Funct. Mater.*, 2004, **14**, 1124-1128.

35 H. Xin, S. Z. Saricilar, H. R. Brown, P. G. Whitten and G. M. Spinks, *Macromolecules*, 2013, **46**, 6613-6620.

36 L. Tan, Y. Liu, W. Ha, L. S. Ding, S. L. Peng, S. Zhang and B. J. Li, *Soft Matter*, 2012, **8**, 5746-5749.

37 Y.H. Na, T. Kurokawa, Y. Katsuyama, H. Tsukeshiba, J. P. Gong, Y. Osada, S. Okabe, T. Karino and M. Shibayama, *Macromolecules*, 2004, **37**, 5370-5374.

38 S. Liang, Z. L. Wu, J. Hu, T. Kurokawa, Q. M. Yu and J. P. Gong, *Macromolecules*, 2011, **44**, 3016-3020.

39 Z. L. Wu, D. Sawada, T. Kurokawa, A. Kakugo, W. Yang, H. Furukawa and J. P. Gong, *Macromolecules*, 2011, **44**, 3542-3547.

40 Q. Chen, L. Zhu, L. Huang, H. Chen, K. Xu, Y. Tan, P. Wang and J. Zheng, *Macromolecules*, 2014, **47**, 2140-2148.

41 R. H. Schmedlen, K. S. Masters and J. L. West, *Biomaterials*, 2002, **23**, 4325-4332.

42 A. K. Gaharwar, S. A. Dammu, J. M. Canter, C. J. Wu and G. Schmidt, *Biomacromolecules*, 2011, **12**, 1641-1650.

43 R. Hou, G. Zhang, G. Du, D. Zhan, Y. Cong, Y. Cheng and J. Fu, *Colloids Surf. B*, 2013, **103**, 318-325.

A graphical and textual abstract

A novel physically linked double-network (DN) hydrogel was prepared based on natural polymer KGM and synthetic polymer PAAm. The DN hydrogels exhibit good mechanical properties, good cell adhesion property, and a unique free-shapeable property, endowing such soft materials promising hydrogels for tissue engineering scaffold.